Signal Dependent Local Noise Removal Using Weiner Filter Decomposition

P Nagarathna[1], Afreen Kubra[2], G. Tirumala Vasu[3], Deepti Raj[4], Anitha Suresh[5], Samreen Fiza[6*]

[1] Department of Computer Science and Engineering, Nitte Meenakshi Institute of Technology, Bengaluru 560064, Karnataka, India
[2] Department of Artificial Intelligence and Machine Learning, HKBK College of Engineering, Bangalore 560045, Karnataka, India
[3,6] Department of Electronics & Communication Engineering, Presidency University, Bangalore 560064, Karnataka, India
[4,5] Department of Electronics & Telecommunication Engineering, Dayananda Sagar College of Engineering, Bangalore 560078, Karnataka, India

[1]nagaratna.p@nmit.ac.in,[2]afreenkubra96@gmail.com,[3]sietk81nitt@gmail.com,[4]deepthiveeraraju@gmail.com,[5]anitha-tce@dayanandasagar.edu, [6*]samreenfiza236@gmail.com

Abstract. Image denoising finds applications in various fields like remote sensing, photography, biological imaging, astronomy etc. If image is corrupted with single source of noise, then a suitable denoising filter can be used. The major challenge associated with image denoising algorithms is denoising of image corrupted with multiple sources of the noise. Excessive smoothing can arise during the reduction of Additive White Gaussian Noise (AWGN) which can lead to a reduction in the level of detail and structural information and if Poisson noise is removed, then the AWGN components will still be retained in resultant image. To address this issue, we propose the Poisson Unbiased Risk Estimate Linear Expansion of Thresholds (PURE LET) approach that denoises mixed AWGN and Poisson noise images using Weiner filter decomposition. The application of a linear transformation to a filtered image allows for an inaccurate computation of the signal dependent local noise variance in the transform domain. Weiner filter inverts the blur of the image and removes extra noise by decomposing. The quantitative and qualitative analysis was conducted to determine the proposed algorithm's efficacy.

Keywords: Image denoising, Weiner filter, PURE LET deconvolution, mixed Poisson-Gaussian noise, BRISQUE, NIQE, PIQE.

1   Introduction

The purpose of denoising an image is to restore the original form of an image from noisy observations. Denoising of an image is a crucial undertaking aimed at rectifying

imperfections that arise during the capture of a real-world scene and its subsequent display, owing to inherent physical and technological constraints. Additionally, it might be advantageous as a preprocessing step to enhance the outcomes of more advanced image processing applications such as fusion [1, 2, 3, 4, 5, 6], object recognition [7, 8, 9, 10, 11], and tracking [12], image registration [13] among others.

During the acquisition process, two primary sources of noise are commonly taken into account. One is due to the presence of intrinsic thermal and electrical fluctuations in acquisition equipment which is a common source, often described by Additive White Gaussian Noise (AWGN) model. The other source arises from variations in the quantity of photons observed, which is an intrinsic constraint of the detecting mechanism employed in photosensitive apparatus, such as Charge-Coupled Device (CCD) cameras, photodiodes and the Photomultiplier Tube (PMT). This commonly occurs under unfavorable circumstances, such as surroundings with inadequate illumination or when exposure times are short. In the framework of photon-counting, Poisson statistics is adhered by noise model, that exhibits a notable dependence on the signal strength. When dealing with images obtained from CCD cameras, the noise is regarded as a composite Poisson-Gaussian model. Low-intensity signals are commonly seen in several fields such as astronomy, medicine, and biology.

The issue of mitigating image noise while retaining its primary attributes, such as edges, textures, colors, and contrast, has been the subject of substantial research in recent decades, resulting in the development of several methodologies. In a nutshell, denoising algorithms can be categorized into three primary groups namely spatial and transform domain methods, and the hybrid ones.

Spatial domain approaches, sometimes referred to as spatial filters, employ a technique wherein the estimation of each pixel is achieved by calculating the weighted average of its neighboring pixels, both local and non-local. The determination of these weights is based on the similarities between the pixels. There exist multiple non-linear as well as linear filter-based techniques, including the Median filter, Wiener filter, Bilateral Filter, Anisotropic Filter, and Total Variation approach, employed for the purpose of eliminating noise from images. Nevertheless, these techniques frequently lead to the undesirable occurrence of the staircase effect and the degradation of structural details. In contrast to the local smoothing filters discussed earlier, the Non-Local Means (NLM) based approaches were initially proposed by Buades et al. [14] with the aim of utilizing the non-local self-similarity present in spatial patterns within real images in order to effectively remove noise. In recent times, a number of variations of the NLM algorithm have been put forth with the aim of enhancing the flexibility and adaptability of non-local filters. Nevertheless, NLM approaches fail to incorporate past knowledge regarding local image structures.

In contrast to spatial domain approaches, transform-based methods have the advantage of facilitating a more straightforward separation of noise and signal. It is assumed that the image can be represented in a sparse manner using certain bases of representation, like the wavelet basis. The methods based on transform domain are commonly employed for wavelet coefficients computation in images and for subsequent reconstruction of these images through the utilization of inverse transformation. While wavelet basis and a few transform domain-based approaches that rely on fixed bases

have demonstrated exceptional denoising capabilities, the utilization of a fixed basis to indicate all local structures often leads to the introduction of visual artifacts. Several approaches based on sparse representation have been presented in order to address the limitations. The fundamental premise underlying the use of sparsity priors is the notion that image patches can be expressed in a sparse manner by a learned dictionary or a fixed basis. Nevertheless, these methodologies typically entail the resolution of an intricate optimization problem and the manually adjustment of parameters in order to approximate the optimal level of performance.

In the recent past, notable progress has been made in the development of hybrid methods that combine spatial domain and transform domain approaches. The hybrid approaches, particularly those using Low-Rank Matrix Approximation (LRMA), have garnered significant attention in image processing area. LRMA focuses on recovering the underlying low-rank matrix structure from noisy observations, making it a popular and effective approach. An exemplary approach, known as Weighted Nuclear Norm Minimization (WNNM), has demonstrated exceptional performance by allotting distinct weights to different singular values. The SAIST technique, employs Singular Value Decomposition (SVD) to sparsely represent image patches. It reduces noise present in an image with the help of an iterative process of singular value shrinkage using the BayesShrink. Zha et al. [15] have proposed a range of image restoration algorithms that leverage a low-rank prior, resulting in notable advancements in this field. The patch-based low-rank image restoration techniques proposed by Guo et al. [16] demonstrate exceptional performance.

In the past few years, there seems to be an increase in the emergence of novel methodologies for image denoising that are built on deep learning, as posited by numerous researchers. This approach involves training image models using large datasets and subsequently utilizing these trained models for the purpose of image denoising. Nevertheless, deep learning techniques strongly depend on the availability of training data, necessitate substantial computational resources, and involve extensive computation. Moreover, they frequently exhibit a noticeable decline in denoising efficacy when confronted with disparities between the images used for training and those used for testing.

The image denoising methods discussed earlier, including traditional methods such as spatial domain and frequency domain, as well as more contemporary deep learning methodologies encounter the challenge of effectively restoring image details and structures with higher precision. Hence, the objective of a denoising method is to preserve a maximal amount of information while effectively eliminating noise present in an image. In this article, a unique denoising model which utilizes the Poisson Unbiased Risk Estimate Linear Expansion of Thresholds (PURE LET) deconvolution approach to effectively eliminate both AWGN and Poisson noise is proposed.

The next few sections of this article are organized as follows. Section II of this manuscript presents a concise overview of the PURE LET deconvolution approach and the proposed algorithm for imagine denoising. In Section III, experimental findings are presented and we illustrate the advantages of the proposed methodology through the evaluation of quality metrics and subjective assessments. In Section IV, this paper is brought to a conclusion and the potential areas for future research are emphasized.

2   Proposed Image Denoising Method

Consider a linear degradation model [17, 18] given by equation (1).

$$y = \alpha P \left(\frac{Hx}{\alpha} \right) \tag{1}$$

where, $y \in R^N$ represents the distorted measurement of the unknown true image $x \in R^N$ which exists in a d-dimensional space and $N = N_1 \times N_2 \times \ldots \times N_d$, $H \in R^{N \times N}$ represents convolution of the Point Spread Function (PSF). The inclusion of $Hx \in R^{N \times N}$ is necessary in order to guarantee the inherent non-negativity of Poisson intensities. $P(.)$ denotes the influence of Poisson noise, and $\alpha \in R_+$ indicates the scaling factor that governs the noise intensity. In particular, higher values of α leads to decreased image intensity, thereby leading to an increase in Poisson noise.

The mathematical expression for the expected value of the Mean Squared Error (MSE) between an estimated value $\hat{x} = F(y)$ and the true value x can be formulated based on the observed image y. Our aim is to determine an estimated value, denoted as $\hat{x}$, which closely approximates the true value, x with the least Mean Squared Error (MSE). Ideally, the objective is to reduce the MSE as represented by equation (2).

$$MSE = \frac{1}{N} E\{\|\hat{x} - x\|^2\} = \frac{1}{N} E \left\{ \sum_{n=1}^{N} (\hat{x}_n - x_n)^2 \right\} \tag{2}$$

where, $E(.)$ represents the mathematical expectation operator.

Let $F(y) = [f_n(y)]_{n=1,2,\ldots N}$ represent a N-dimensional real-valued vector function. Assuming the invertibility of equation (1) and the invertibility of H, the random variable $PURE\{F\}$ can be expressed by equation (3).

$$PURE\{F\} = \frac{1}{N} \|F(y)\|^2 - \frac{2}{N} y^T H^{-T} F^-(y) + \varepsilon_P \tag{3}$$

where, $PURE\{F\}$ represents an unbiased estimate of the expected MSE indicated by equation (4).

$$E\{PURE\} = \frac{1}{N} E\{\|F(y) - x\|^2\} \tag{4}$$

where, $F^-(y) = [f_n(y) - \alpha e_n]_{n=1,2,\ldots N}$ e_n is the N-dimensional vector with components δ_{k-n} ; $k = 1,2,\ldots N$, $\varepsilon_P = (y^T H^{-T} H^{-1} y - \alpha 1^T H^{-T} H^{-1} y)/N$ is independent on F.

The absence of bias between MSE and $PURE$, together with a high N value, suggests that equation (3) can serve as a dependable alternative to the MSE. This is supported by the law of large numbers, which states that a sample mean, such as MSE and $PURE$, converges to its mathematical expectation. In practical applications, all elements can be

computed due to the substitution of the MSE with a statistical counterpart that elimi-nates its dependence on variable x.

The observed noisy image is passed through Weiner filtering which is then followed by denoising in the transform domain of the decomposed images. A suitable sub-band adaptive thresholding is applied to obtain reconstructed images. The estimate $\hat{x}$ is de-rived by reducing the reconstructed images using PURE LET approach as depicted in Fig 1.
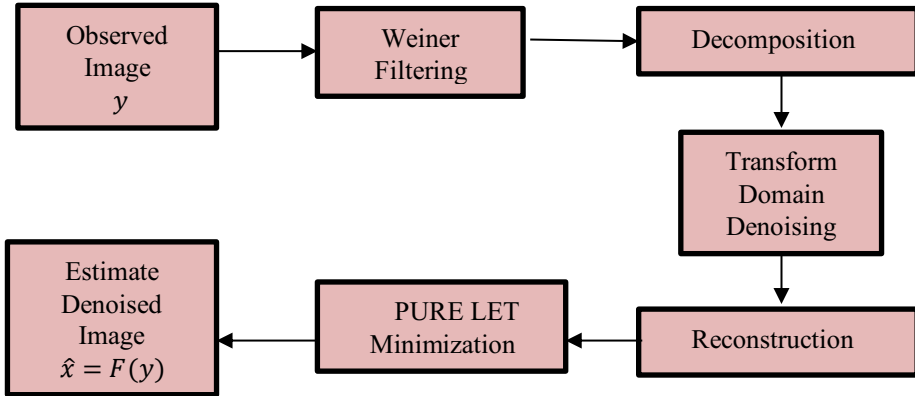

Fig 1. Block diagram of the image denoising technique using PURE LET

3   Result Analysis

The proposed denoising algorithm is tested on images taken from dataset [19, 20]. These test samples are manually added with AWGN and Poisson noise with scaling factor α set to 0.9 to 0.99 which indicates that the ground truth images are 90 to 99 percent corrupted by noise as shown in left side images of Fig 2. The middle column of Fig 2 represents the denoised images using PURE LET approach. The last column of Fig 2 indicates the ground truth data. It is very clear that the subjective assessment of the proposed algorithm has denoised the noisy samples efficiently.

(i) Noisy test sample 1   (ii) Output denoised image   (iii) Ground truth
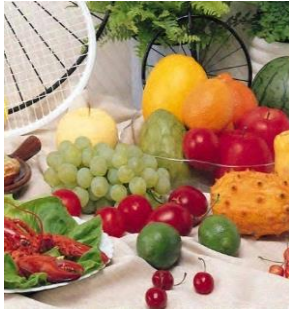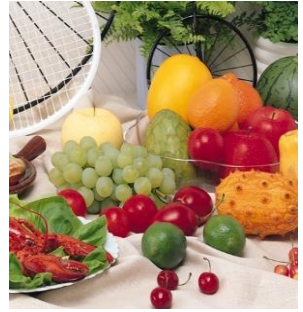
(iv) Noisy test sample 2   (v) Output denoised image   (vi) Ground truth

(vii) Noisy test sample 3   (viii) Output denoised image   (ix) Ground truth

(x) Noisy test sample 4   (xi) Output denoised image   (xii) Ground truth

(xiii) Noisy test sample 5   (xiv) Output denoised image   (xv) Ground truth
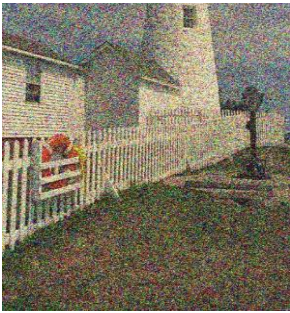
(xvi) Noisy test sample 6   (xvii) Output denoised image   (xviii) Ground truth

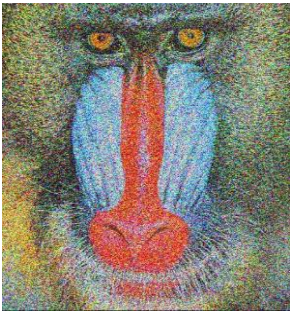
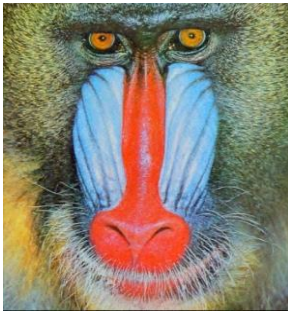(xxi) Noisy test sample 7   (xx) Output denoised image   (xxi) Ground truth
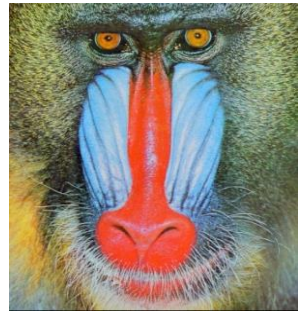

(xxii) Noisy test sample 8   (xxiii) Output denoised image   (xxiv) Ground truth

(xxv) Noisy test sample 9   (xxvi) Output denoised image   (xxvii) Ground truth

(xxviii) Noisy test sample 10   (xxxi) Output denoised image   (xxx) Ground truth

Fig 2. Result analysis of the proposed PURE LET deconvolution image denoising approach

The effectiveness of the proposed algorithm in this manuscript has been objectively evaluated through the utilization of various metrics, including Perception-based Image Quality Evaluator (PIQE), Peak Signal-To-Noise Ratio (PSNR), Naturalness Image Quality Evaluator (NIQE), and Blind/ Referenceless Image Spatial Quality Evaluator (BRISQUE).

PSNR is a quantitative measure that compares the maximum signal power to the distorting noise power, which ultimately impacts the quality of image representation. PSNR is a extensively employed metric for quantifying the quality of image reconstruction in the presence of various levels of noise. BRISQUE is a natural scene statistic-based evaluator that utilizes local normalized luminance signals to extract point-wise statistics. It assesses the naturalness of an image by measuring the deviations from a natural image model. NIQE is founded on the development of a statistical feature set that is "quality aware" which is derived from a straightforward and effective space domain model known as Natural Scene Statistic (NSS). The aforementioned features are obtained by the utilization of a corpus consisting of undistorted, natural images. The quality assessment methodology employed by PIQE involves the utilization of a block-wise technique to evaluate the quality of a given image, taking into consideration an arbitrary form of distortion.

BRISQUE, NIQE, PIQE are image quality scores with no reference image. A lower score is indicative of superior perceptual quality. High PSNR and low BRISQUE, NIQE, and PIQE metric values are preferred to prove the efficiency of the algorithm.

As shown in Table 1, for test samples 1 and 2, α is set to 0.90, which leads to their PSNR metric values to a high value equal to 32.31608 and 29.43789, BRISQUE metric is reduced by 50 % of its input value, similarly NIQE is reduced to 80% of its input value, and PIQE is reduced to 65% of its input value. As explained earlier high PSNR and lower BRISQUE, NIQE, PIQE are preferred.

For test samples 3 and 4, α is set to 0.99, even though the noise level is highest in this sample, PSNR value is almost same as that of test sample 1 and 2. Similar variations in remaining metrics can be observed. Since the efficiency of the algorithm can be tested based on noise levels, the proposed algorithm has been tested for noise levels

starting from 90% to 99% noise corrupted images, and we have obtained good metric values.

Table 1. PSNR, BRISQUE, NIQE, PIQE metric value for the noisy test samples and corresponding denoised images

Noisy Test Sample	Input PSNR	Output PSNR	Input BRISQUE	Output BRISQUE	Input NIQE	Output NIQE	Input PIQE	Output PIQE
1	22.18645	32.31608	41.77687	21.83309	10.32165	2.468435	57.77892	26.72876
2	22.40793	29.43789	37.25678	24.38887	8.668735	2.397657	56.33961	11.16012
3	22.53987	28.00275	36.54491	26.81331	11.39234	3.06424	50.64443	13.00266
4	22.17224	31.27656	41.74883	33.68759	12.87197	6.185475	60.88644	25.77333
5	22.33087	29.26785	37.17823	22.89366	8.619324	4.180946	50.46461	32.9536
6	22.24332	31.92569	40.64315	29.73407	11.15319	2.906624	58.43003	31.67095
7	22.24459	30.34808	42.23467	25.38265	10.57013	2.484496	58.34107	22.77775
8	22.21786	26.67505	41.34621	22.90291	9.301183	3.921342	61.8011	32.14361
9	22.27805	34.02164	41.57237	24.29464	11.28927	4.092291	64.2139	26.55424
10	22.33342	30.7253	40.38109	22.38636	12.34342	3.875918	59.98048	23.57291

In Fig 3, graphical illustration of quality metrics PSNR, PIQE, NIQE and BRISQUE is shown for better interpretation of results. The vertical axis of the graph depicts the ten noisy image samples, while the horizontal axis represents the corresponding metric values. The output denoised images have higher PSNR and lower BRISQUE, NIQE and PIQE compared to input noisy images.
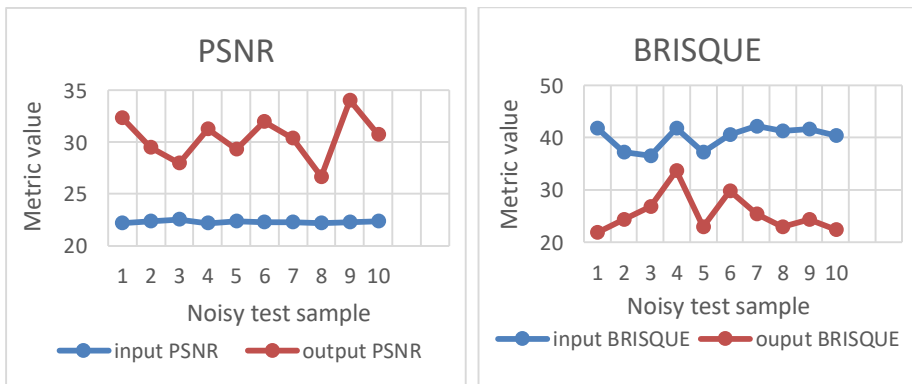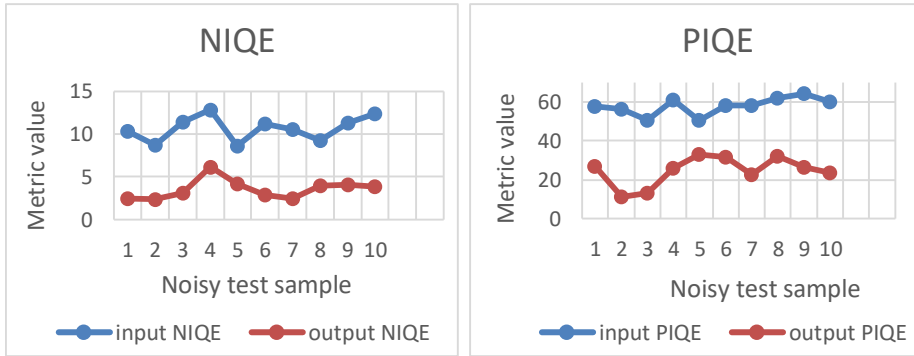
Fig 3. Graphical representation of performance metrics

4   Conclusion and Scope for Future Work

A novel signal dependent local noise removal technique that uses Weiner filter decomposition is proposed. As images are affected with multiple sources of noise say mixed AWGN and Poisson noise, our algorithm can effectively denoise using Poisson Unbiased Risk Estimate Linear Expansion of Thresholds (PURE LET) approach. The method that has been proposed in this article demonstrates superior performance with respect to the quality of restoration. The efficiency of the proposed method is assessed by the utilization of various metrics, such as Peak Signal-to-Noise Ratio (PSNR), Blind/Referenceless Image Spatial Quality Evaluator (BRISQUE), Naturalness Image Quality Evaluator (NIQE), and Perception-based Image Quality Evaluator (PIQE).

References

[1]   G. Tirumala Vasu; P. Palanisamy, "CT and MRI multi-modal medical image fusion using weight-optimized anisotropic diffusion filtering," *Soft Computing,* vol. 27, no. 13, p. 9105–9117, 2023.

[2]   G. Tirumala Vasu; P. Palanisamy, "Gradient-based multi-focus image fusion using foreground and background pattern recognition with weighted anisotropic diffusion filter," *Signal, Image and Video Processing,* vol. 17, no. 5, p. 2531–2543, 2023.

[3]   G. Tirumala Vasu and P. Palanisamy , "Multi-focus image fusion using anisotropic diffusion filter," *Soft Computing,* vol. 26, no. 24, pp. 14029-14040, 2022.

[4]   G. T. Vasu and P Palanisamy, "Visible and Infrared Image Fusion Using Distributed Anisotropic Guided Filter," *Sensing and Imaging,* vol. 24, no. 1, pp. 1-17, 2023.

[5]   S. Fiza and S. Safinaz, "Multi-focus image fusion using edge discriminative diffusion filter for satellite images," *Multimedia Tools and Applications,* pp. 1-20, January 2024.

[6]   G. Tirumala Vasu and P. Palanisamy, "Multi-exposure image fusion using structural weights and visual saliency map," *Multimedia Tools and Applications,* 2024.

[7]   A. Kubra, S. Tatekalva, A. K. Kumar, G. T. Vasu and S. Fiza, "DEEP LEARNING ALGORITHMS BASED SKIN DISEASE DETECTION AND CLASSIFICATION," *Journal of Cardiovascular Disease Research,* vol. 12, no. 7, pp. 2472-2482, 2021.

[8]   Sandhya Tatekalva, Kishore Kumar, G. Tirumala Vasu and Samreen Fiza, "Pneumonia Detection Using Deep Learning Model," *Solid State Technology,* vol. 61, no. 4, pp. 184-191, 2018.

[9]   G. T. Vasu, S. Fiza, A. Kubra, A. K. Kumar and K. Seelam, "DEEP LEARNING MODEL BASED EARLY PLANT DISEASE DETECTION," *NeuroQuantology,* vol. 20, no. 20, pp. 1818-1824, 2022.

[10]   G. T. Vasu, S. Fiza, S. Tatekalva and K. Kumar, "Deep Learning Model based Object Detection and Image Classification," *Solid State Technology,* vol. 61, no. 3, pp. 15-25, 2018.

[11]   S. Fiza, G. T. Vasu, A. Kubra, A. K. Kumar and K. Seelam, "MACHINE LEARNING ALGORITHMS BASED SUBCLINICAL KERATOCONUS DETECTION," *NeuroQuantology,* vol. 20, no. 20, pp. 1825-1837, 2022.

[12]   S. Fiza, "ALGORITHMIC DEVELOPMENT AND DESIGN," in *Feature Extraction and Gesture Recognition*, COUNCIL OF INDUSTRIAL INNOVATION AND RESEARCH (CIIR), 2023, p. 10.

[13]   P. Nagarathna, A. Jeelani, S. Fiza, G. T. Vasu and K. Seelam, "Medical Image Registration with Object Deviation Estimation through Motion Vectors using Octave and Level Sampling," *Automatika,* vol. 65, no. 3, pp. 1213-1227, 2024.

[14]   B. A., C. B. and M. J.-M, "A non-local algorithm for image denoising," in *2005 IEEE Computer Society Conference on Computer Vision and Pattern Recognition*, 2005.

[15]   Z. Z., Y. X., Z. J., Z. C. and W. B., "Image restoration via simultaneous nonlocal self-similarity priors," *IEEE Transactions on Image Processing,* vol. 29, pp. 8561-8576, 2020.

[16]   G. Q., G. S., Z. X., Y. Y. and Z. C., "Patch-based image inpainting via two-stage low rank approximation," *IEEE transactions on visualization and computer graphics,* vol. 24, no. 6, pp. 2023-2036, 2017.

[17]   S. Lefkimmiatis and M. Unser, "Poisson Image Reconstruction With Hessian Schatten-Norm Regularization," *IEEE Transactions on Image Processing,* vol. 22, no. 11, pp. 4314-4327, 2013.

[18]   Z. T. Harmany, R. F. Marcia and R. M. Willett, "This is SPIRAL-TAP: Sparse Poisson Intensity Reconstruction ALgorithms—Theory and Practice," *IEEE Transactions on Image Processing,* vol. 21, no. 3, pp. 1084-1096, 2012.

[19]   A. Weber, "The USC-SIPI Image Database," USC VITERBI, School of Engineering, [Online]. Available: https://sipi.usc.edu/database/database.php?volume=misc.

[20]   E. Vrscay, F. Mendivil, H. Kunze, D. L. Torre and S. Alexander, "The Waterloo Fractal Coding and Analysis Group," [Online]. Available: https://links.uwaterloo.ca/Repository.html.